Ornamental Plant Research

ARTICLE

Open Access

https://doi.org/10.48130/opr-0025-0052

Ornamental Plant Research **2026**, 6: e010

Physiological responses and screening of key genes involved in the cold tolerance of herbaceous peony cultivated over-winter in Harbin, the coldest metropolis of China

Yan Shen[1], Qiyao Wang[1], Danqing Li[2], Xiaohua Shi[3], Xiaoxuan Chen[1], Junhong Guo[1], Yiping Xia[1], Zhiyang Liu[4,5*] and Jiaping Zhang[1*]

[1] *College of Agriculture and Biotechnology, Zhejiang University, Hangzhou 310058, China*
[2] *College of Civil Engineering, Zhejiang Sci-Tech University, Hangzhou 310018, China*
[3] *Zhejiang Institute of Landscape Plants and Flowers, Zhejiang Academy of Agricultural Sciences, Hangzhou 311251, China*
[4] *College of Life Sciences, Northeast Forestry University, Harbin 150040, China*
[5] *Institute of Horticulture, Harbin Academy of Agricultural Sciences, Harbin 150029, China*
* Correspondence: liuzhiyanger@126.com (Liu Z); zhangjiaping0604@aliyun.com (Zhang J)

Abstract

Herbaceous peony is a globally-renowned ornamental plant. Extreme winter conditions can severely damage the underground buds and crowns, and hinder subsequent bud break and growth of herbaceous peony, although it has a certain degree of cold tolerance. This study offers new insights into the cold tolerance of herbaceous peony by comparing two cultivars of contrasting provenances and tolerances to cold. Physiological observation, transcriptome sequencing, and gene expression analysis were performed on overwintering crown buds exposed to freezing conditions in Harbin. The two cultivars demonstrated relatively significant morphological and physiological differences in response to cold stress. Specifically, HL exhibited superior morphological traits, including more stems (4.30 vs 3.47) and flowers (12.67 vs 5.87) per plant, as well as significantly higher soluble sugar content (e.g., 280 mg/g FW vs 210 mg/g FW in January). Transcriptome results show that various expressed genes were in connection with starch and sucrose metabolism, plant-pathogen interactions, and phytohormone signaling pathways. The co-expression analysis identified and visualized the key genes in the two modules, ME black and ME yellowgreen. Integrating physiological changes with expression of genes, several key genes were identified, such as *XERO1*, *LTI65*, *NADP-ME4*, *WRKY39*, and *ASA2*, which are probably involved in the cold-stress response, and thus deserve further exploration in gene function and interaction. This study provides new insight into the cold-tolerance of herbaceous peony and paves the way for its future studies, and also contributes to breeding strong cold-resistant cultivars of herbaceous peony in the high-latitude regions with harsh winters.

Citation: Shen Y, Wang Q, Li D, Shi X, Chen X, et al. 2026. Physiological responses and screening of key genes involved in the cold tolerance of herbaceous peony cultivated over-winter in Harbin, the coldest metropolis of China. *Ornamental Plant Research* 6: e010 https://doi.org/10.48130/opr-0025-0052

Introduction

Cold stress, encompassing chilling stress (0–15 °C) and freezing stress (< 0 °C), represents a significant abiotic stress causing substantial economic losses in horticultural crops[1,2]. Typical damage induced by cold temperatures includes impaired photosynthesis, decreased cell membrane fluidity leading to rigidity, destabilization of proteins and protein complexes, and even cell death due to dehydration[3]. These effects restrict the geographical distribution of plant species and reduce global crop yields, creating worldwide negative impacts on plant systems. The compounded effects of membrane dysfunction, protein denaturation, and structural collapse under cold stress collectively threaten sustainability across diverse ecosystems[4–6].

Plants have evolved sophisticated regulatory mechanisms to withstand cold stress, such as synthesizing various protective compounds and proteins, including soluble sugars, proline (PRO), cold-resistant proteins, phytohormones, and epigenetics. These substances participate in regulating osmotic potential and cell membrane stability in plants under cold stress[7]. Additionally, plants activate antioxidant systems by enhancing the activities of enzymes like superoxide dismutase (SOD) and peroxidase (POD), which contribute to reactive oxygen species (ROS) scavenging[4]. For instance, wheat (*Triticum aestivum* L.) enhances its antioxidant defense to improve cold resistance, while bamboo (Bambusoideae) and aloe vera (*Aloe vera* [L.] Burm. f.) boost activities of SOD and POD to elevate amino acid and soluble sugar levels, mitigating cold-induced damage[8,9]. Furthermore, plants adapt to cold environments through dynamic adjustments in phytohormone levels and balances that modify growth patterns[10]. Phytohormones such as abscisic acid (ABA) and jasmonic acid (JA) play critical roles in cold adaptation across species like wheat and apple (*Malus domestica* Borkh.)[11,12]. The synergistic integration of physiological regulation and metabolic reprogramming constitutes a fundamental adaptive strategy that enables plants to withstand freezing environments[13]. Plants are also able to modify translation efficiency and methylation status through epigenetics, thereby enhancing cold tolerance via non-nucleotide sequence changes such as structural alterations.

Research on the plant cold tolerance involves morphological observation, physiological measurement, omic sequencing, and bioinformatics-related analysis, and the subsequent identification of crucial genes[14]. Screening of cold-resistant genes is a pivotal component in such research, bridging a series of studies at morphological, physiological, proteomic, and omics levels, and thus it paves the way for subsequent investigations into gene function and interaction[15]. Multiple methodologies exist for screening cold-resistant genes. Current mainstream approaches focus on correlating morphological and physiological observations with gene expression data acquired by transcriptome through the weighted gene co-expression network analysis (WGCNA). Adverse

environmental conditions activate stress-responsive gene expression through complex signaling pathways. This activation leads to downstream physiological and biochemical adaptations, which makes transcriptomics a key tool for studying stress-related gene expression. This method has been frequently applied in crops such as rice and upland cotton (*Gossypium hirsutum* L.)[16,17].

Herbaceous peony (*Paeonia lactiflora* Pall.) is a world-famous ornamental valued for beautiful flowers, elegant leaves, and medicinal and edible oil uses. It exhibits relatively weak heat tolerance. Therefore, most researches focus on the southward introduction, cultivation adaptability, and heat resistance mechanisms of herbaceous peony[18–21]. However, the cultivation of this ornamental in high-latitude regions like Northeast China also remains limited. The primary constraint lies in the extreme winter conditions of areas such as Heilongjiang Province, where temperatures routinely plunge −30 °C below, creating deep frozen soil layers. The mechanical stress and cellular dehydration of herbaceous peony's buds and crowns under frozen ground disrupt meristematic tissues, and thus lead to compromised spring sprouting, stunted growth, floral abortion, and low flowering rate[22]. Despite some preliminary research exploring cold resistance in herbaceous peony, a critical knowledge gap persists due to the insufficient systematic investigations integrating physiological, biochemical, and transcriptomic analyses[23]. Additionally, previous studies on herbaceous peony cold tolerance also exhibit several other limitations. These include insufficient comparative analyses between low-latitude and high-latitude germplasms and inadequate investigation of tender underground bud organs beneath frozen soil. There is also an incomplete identification of key regulatory genes with limited genetic resources. Therefore, understanding how herbaceous peony crown buds perceive low temperatures and coordinate genetic regulation is crucial[24].

In this study, two representative herbaceous peony cultivars with contrasting cold-resistances from distinct southern and northern Chinese production regions were selected to explore the physiological regulation of cold-tolerance and mine the crucial associated genes. The study features three novel aspects: comparison of cultivars from totally different climatic regions, conducting experiments in the northernmost Chinese metropolis, and focusing on bud survival under frozen soil instead of traditional research on the aboveground part. This study offers novel insights into plant cold-adaptation mechanisms in extreme high-latitude cold regions. It lays important groundwork for future functional and interaction studies of cold-tolerance genes in herbaceous peonies, and also provides theoretical support for breeding strong cold-resistant herbaceous peony cultivars. These new cultivars could be planted and used in the high-latitude regions.

Materials and methods

Plant materials

Two representative cultivars with contrasting provenance and cold tolerance were selected as experimental materials: 'Hang Baishao' (hereafter abbreviated as HB), an herbaceous peony cultivar originating from the lowest latitude region in China[24]. and 'Hongling Chijin' (hereafter abbreviated as HL), a cold-resistant cultivar of northern origin, identified through introduction and screening in Harbin (44°04′~ 46°40′ N, 125°42′~ 130°10′ E) (Fig. 1a, b, and Table 1). These two were introduced to the open experimental nursery of the Harbin Academy of Agricultural Sciences in Songbei District, Harbin, Heilongjiang Province, China. Daily temperatures during the period from November 2022 to January 2023 are all shown in Fig. 1c–e, and the temperature data referenced in this analysis are accessible at https://tianqi.2345.com/. The buds of two cultivars in the underground frozen soil layer were sampled on November 10, 2022, December 10, 2022, and January 10, 2023. Three biological replicates per cultivar were collected at each sampling stage. All samples were immediately frozen in liquid nitrogen and stored at −80 °C for subsequent experiments.

Morphological observations for budbreak and growth after an extremely cold winter in Harbin

Plant height, stem width, bud height, and bud diameter were collected using standardized measuring tapes. Plant height was measured vertically from the substrate to the tallest leaf apex. Stem width was assessed at the main stem base, and bud dimensions were recorded at their median points to ensure representative sampling. Based on previous studies on the comprehensive adaptive evaluation of herbaceous peony, the flower number per plant, i.e., the number of fully bloomed flowers, was confirmed during the peak flowering stage[25,26].

Physiological and biochemical assays

Soluble sugar contents were determined using a Soluble Sugar Content Assay Kit (Bixbio, Beijing, China). Soluble protein concentrations were measured with a Bradford Protein Assay Kit (Beyotime, Shanghai, China). Stress-related enzyme activities and proline (PRO) contents were quantified using specific detection kits: peroxidase (POD) Assay Kit, superoxide dismutase (SOD) Assay Kit, and Proline Assay Kit (all from Jiancheng, Nanjing, China). Phytohormone levels in buds were analyzed via the enzyme-linked immunosorbent assay (ELISA), targeting nine phytohormones across five categories: abscisic acid (ABA); auxins: indoleacetic acid (IAA) and indolepropionic acid (IPA); gibberellins (GA_3 and GA_4); cytokinins: zeatin riboside (ZR) and dihydrozeatin riboside (DHZR); brassinolide (BR); and methyl jasmonate (MeJA)[27].

RNA extraction, cDNA synthesis, and quality assessment

Total RNA was extracted from both cultivars using the EASYspin Plus Complex Plant RNA Kit (RN53, Aidlab, Beijing, China). Reverse transcription to synthesize cDNA was performed with the PrimeScript™ RT Reagent Kit with gDNA Eraser (Perfect real-time) (RR047A, Takara, Japan). RNA purity and concentration were evaluated using a NanoDrop 2000 spectrophotometer (Thermo SCIENTIFIC, America), while RNA integrity was precisely assessed with a LabChip GX Touch HT system.

Table 1. Detailed information on experimental materials HB and HL.

Cultivar	Location	Latitude	Flower type	Feature
Hang Baishao (HB)	Pan'an, Zhejiang Province	N 28°49′–29°19′	Single-petal type	The Chinese southernmost peony cultivar with weak cold resistance that has been cultivated and produced intensively in Zhejiang for more than 1,000 years
Hongling Chijin (HL)	Heze, Shandong Province	N 44°04′–46°40′	Single-petal type	A cultivar with strong cold resistance that was discovered after being introduced and screened in Harbin, the northernmost metropolis city in China

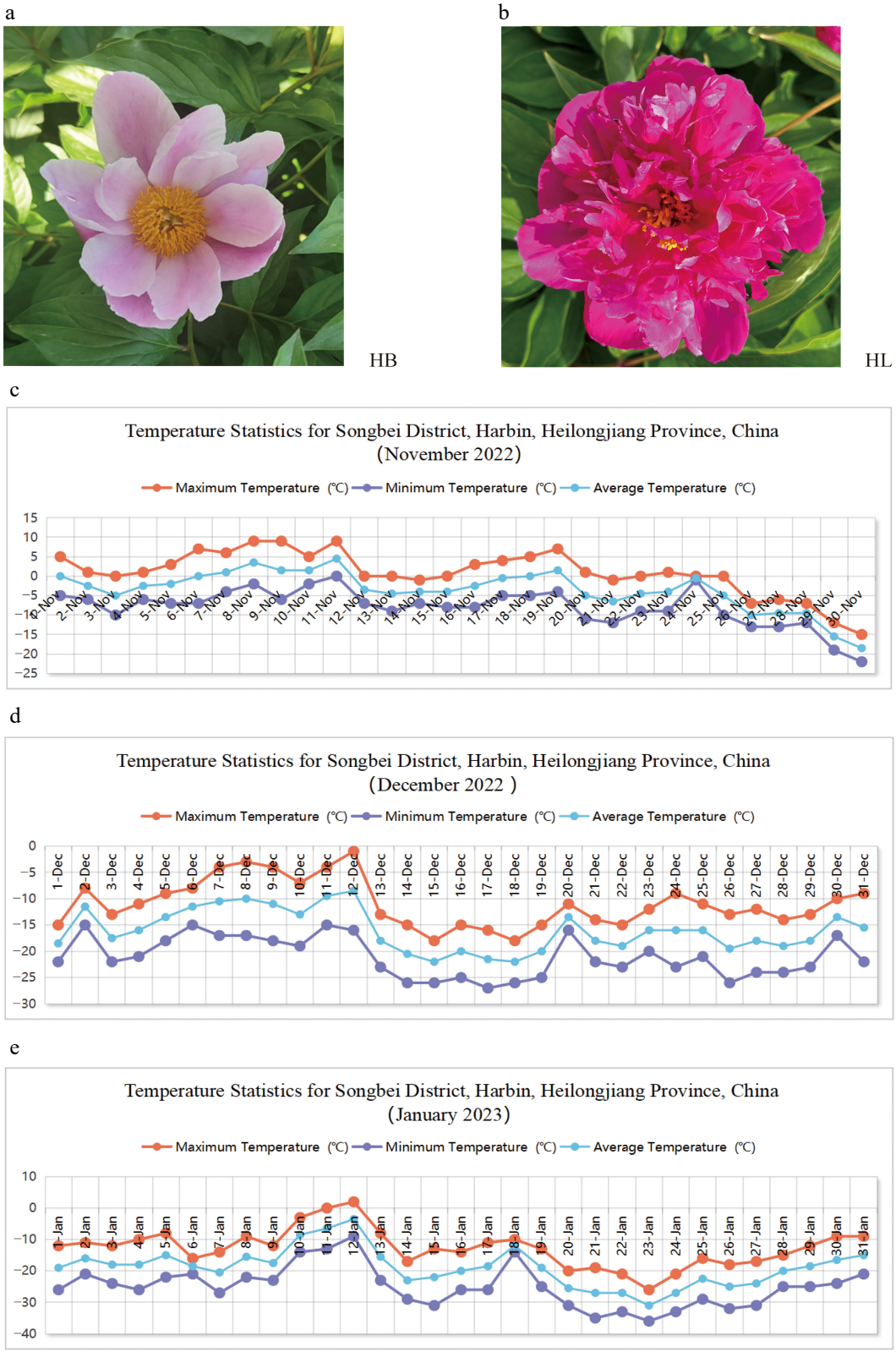

Fig. 1 Experimental materials: (a) 'Hang Baishao' (HB). (b) 'Hongling Chijin' (HL). Temperature statistics for Songbei district, Harbin, Heilongjiang Province, China. (c) November 2022. (d) December 2022. (e) January 2023.

Transcriptome sequencing and annotation

The experimental samples, consisting of three biological replicates each of HB and HL collected during three winter periods (November 2022 to January 2023), were processed for transcriptome analysis. All samples were shipped to the Biomarker Technologies Corporation (Beijing, China) for the transcriptome library construction and sequencing using the Illumina NovaSeq 6000 platform with PE150 sequencing mode. Sequence assembly

was conducted via Trinity (v 2013), yielding 55,498 assembled transcripts (Unigenes or genes). Sequences of these transcripts were aligned against the NCBI non-redundant protein database (NR), Swiss-Prot, Clusters of Orthologous Groups (COG), Eukaryotic Orthologous Groups (KOG), evolutionary genealogy of genes: Non-supervised Orthologous Groups (eggNOG 4.5), and Kyoto Encyclopedia of Genes and Genomes (KEGG) databases by using DIAMOND software. KEGG Orthology (KO) annotations were obtained through KOBAS. Gene Ontology (GO) analysis was performed using InterProScan with integrated InterPro databases. Amino acid sequences of Unigenes were predicted and aligned against the Pfam database via HMMER software to acquire functional annotations.

qRT-PCR and detecting the accuracy of transcriptome Unigene expression levels

To verify the expression trend of transcripts in the transcriptome and investigate expression patterns of selected genes, this study designed primers targeting transcript sequences of candidate genes (Table 2) and performed quantitative expression assays following omics data acquisition. Quantitative real-time PCR (qRT-PCR) was conducted using the NovoStart® SYBR qPCR SuperMix Plus (GenStar BioSolutions, Shanghai, China) on a Bio-Rad CFX96 system (Bio-Rad Laboratories, Shanghai, China). The thermal cycling protocol included: 95 °C for 1 min (initial denaturation); 40 cycles of 95 °C for 20 s (denaturation), 52 °C for 20 s (annealing), and 72 °C for 30 s (extension); followed by a melt curve analysis (95 °C for 5 s, 65 °C for 5 s, and 95 °C for 5 s). The α-Tubulin gene (ATUBA) was used as the reference gene, and relative gene expression levels were calculated using the $2^{-\Delta\Delta C_T}$ method[28,29].

Identification of differentially expressed genes

Differentially expressed genes (DEGs) were identified using DESeq2 with stringent thresholds: p_{adjust} value < 0.001 and $|\log_2$ fold change$|$ > 1. DEGs from different comparison groups were pooled via Venn analysis, followed by time-series clustering using the MFuzz algorithm implemented on the Bioinformatics Online Platform (www.bioinformatics.com.cn). KEGG functional enrichment analysis was performed using TBtools (v2.225)[30].

Adopting the WGCNA to screen the key genes involved in cold tolerance

The WGCNA package in R was employed to construct co-expression networks by integrating morphological and physiological indices measured previously and transcriptomic data from bud samples. Gene modules were correlated with cold resistance-related traits through Pearson correlation coefficients. Key modules demonstrating significant correlations were subjected to KEGG functional enrichment analysis using TBtools (v2.225). Hub genes within these modules were identified and ranked by degree values (a connectivity metric) using Cytoscape (v3.10.1) for the co-expression network visualization[31].

Data analysis

Data processing, statistical analysis, and graphical visualization were performed using Excel (2016), SPSS (v25.0), R (v4.4.1), TBtools (v2.225), Cytoscape (v3.10.1), GraphPad Prism (v10.0), the Bioinformatics Online Platform (www.bioinformatics.com.cn), and the Biomarker Cloud Platform (https://international.biocloud.net). One-way analysis of variance (ANOVA) was used for statistical comparisons, with results expressed as mean ± standard deviation (SD) from at least three biological replicates and statistical significance set at $p < 0.05$.

Results

Morphological observations

As herbaceous perennials, two cultivars exhibited distinct morphological differences. HL demonstrated greater morphological traits compared to those of HB ($p < 0.001$). Specifically, HL exhibited a plant height of 89.70 cm vs 73.24 cm for HB, a crown width of 81.40 cm vs 72.07 cm, 4.30 vs 3.47 stems per plant, and 12.67 vs 5.87 flowers per plant (Fig. 2a–d). HL displayed a more robust growth habit with larger overall plant dimensions and more abundant flowering than HB. Bud length differed significantly between cultivars throughout overwintering stages, with HL exhibiting consistently longer buds than HB (Fig. 2e). Bud diameter showed no significant differences, though HL buds were marginally thicker than HB at each stage (Fig. 2f).

Soluble sugar and protein quantifications

Plants synthesize protective compounds such as soluble sugars and proteins to enhance cold-stress tolerance. Soluble sugar content increased significantly in both cultivars as cold stress intensified from November to January, with HL maintaining significantly higher levels than HB at all time points. For instance, in November, HL contained about 140 mg/g FW compared to 110 mg/g FW in HB; by January, levels rose to approximately 280 mg/g FW in HL vs 210 mg/g FW in HB (Fig. 2g). Soluble protein concentrations remained elevated between 6–7 mg/g FW throughout the sampling periods, with HB showing slightly higher values than HL at each stage (Fig. 2h).

Peroxidase activity assays

Physiological assessments of ROS accumulation and enzymatic scavenging systems revealed distinct patterns between HB and

Table 2. The primers for qRT-PCR.

Abbreviations	Full names	Forward primer sequences (5' to 3')	Reverse primer sequences (5' to 3')
ATUBA	*ABA-Triggered Ubiquitin ligase for Cold Adaptation*	GACGTGGGCTCGATCTGAAT	ATCCCTTGCCTGAGCATCAC
APL	*AQUAPORIN-LIKE PROTEIN*	AGGCGAAGCAGGAATGAAGT	CAACTGACCTGTCACCCGTT
BMY	*β-AMYLASE GENE*	CCAATTGGGGACTTGGTGGT	GCCATGGTTGGTAAAAGCGG
GBSS	*Granule-Bound Starch Synthase*	ATGTTCTAGGGGGACTGCCA	GCACAGCAAGCTGAAACGAA
GRXS17	*GLUTAREDOXIN S17*	ATCTGGTCTTCCCAACACGC	TCAACCCTTCACGAACCTCG
GSH2	*GLUTATHIONE SYNTHETASE 2*	TTGATGCAGAAGGGGAGCTT	GTTGGTGCATACCCAGCTCT
MSD1	*MALONYL-CoA SYNTHETASE DEFECTIVE 1*	CCTATTCGTGAAGGAGGCGG	GGTCCTGATTGGCAGTGGTT
ABF3	*Abscisic Acid-Responsive Element-Binding Factor 3*	GGTTGGTTTAGGACCAGGGG	ATGTACCTGCTTACGAGCCC
IAA9	*Indole-3-Acetic Acid 9*	ACATGAGGAGAAGCCGTTGT	TGAGTGGTGGAAGCCCTAGA
SPY	*SPINDLY*	ACTGGGGTAGGCGCTTTATG	GCATCTGCCTTCACAACTGC

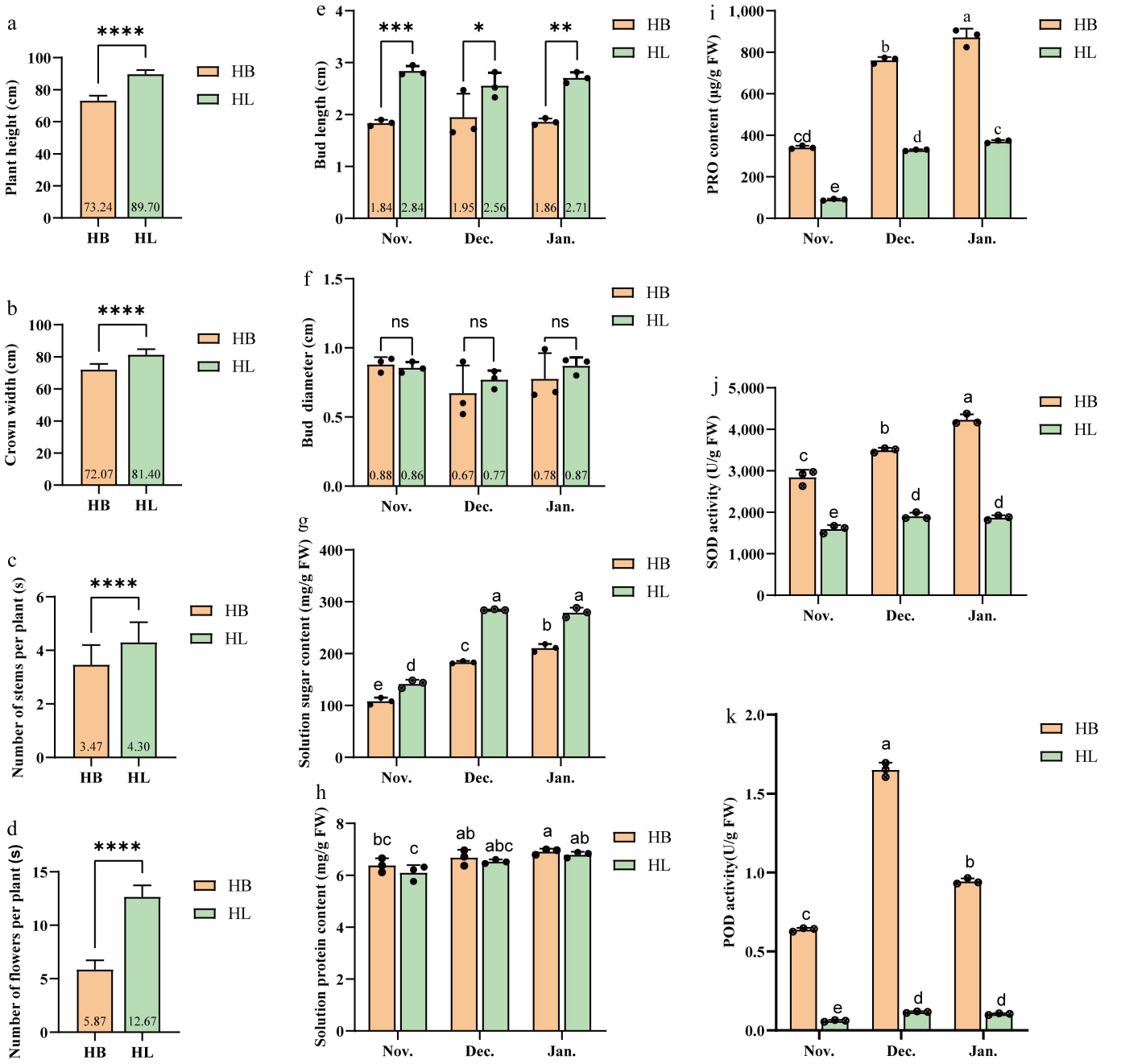

Fig. 2 Morphological and physiological data in 'Hang Baishao' (HB) and 'Hongling Chijin' (HL) during the winter of Harbin. (a) Plant height. (b) Crown width. (c) Number of stems per plant. (d) Number of flowers per plant. (e) Bud length. (f) Bud diameter. (g) Soluble sugar content. (h) Soluble protein content. (i) PRO content. (j) SOD activity. (k) POD activity. All data are the means of three replicates with standard deviations, and different letters indicate significant differences among the data according to Duncan's multiple range test. * indicates significant difference at the 0.05 probability level, ** indicates extremely significant difference at the 0.01 probability level, *** indicates extremely significant difference at the 0.001 probability level, **** indicates extremely significant difference at the 0.0001 probability level, and ns indicates non-significant. Different lowercase letters above the bars of Fig. 2g–k show significant differences at the 0.05 probability level; $n = 3$.

HL. Across all sampling stages, HB exhibited significantly higher PRO, SOD, and POD activities compared to HL (Fig. 2i–k). Throughout the sampling period from November to January, HB consistently showed higher levels of PRO, SOD, and POD activities compared to HL. PRO in HB peaked at approximately 870 μg/g FW in January, significantly above HL's 370 μg/g FW (Fig. 2i). Similarly, SOD activity in HB rose to about 4,200 U/g FW, surpassing the 1,880 U/g FW in HL (Fig. 2j). POD activity in HB exhibited a biphasic pattern, increasing to nearly 1.65 U/g FW in December before declining, while HL maintained stable levels around 0.1 U/g FW (Fig. 2k). Both cultivars exhibited rising PRO accumulation and SOD activity with prolonged cold exposure. Notably, POD activity in HB displayed a biphasic response, initially increasing, followed by a decline, contrasting with the sustained enzymatic profile in HL.

Phytohormone profiling

Dynamic phytohormone fluctuations can reflect plant adaptation to stress. During cold exposure, the eight phytohormones measured

in the HB cultivar exhibited different response patterns. GA_3, IAA, IPA, and DHZR levels exhibited sustained increases throughout the experimental period (Fig. 3b, f, g, i). ABA, GA_4, MeJA, and ZR concentrations displayed biphasic patterns, with initial declines followed by subsequent increases (Fig. 3a, c, d, h). BR levels showed an initial rise followed by a reduction (Fig. 3e). Under identical experimental conditions, the same phytohormones in the HL cultivar exhibited different response patterns. ABA, GA_3, BR, IAA, IPA, ZR, and DHZR levels peaked mid-experiment before declining (Fig. 3a, b, e–i). GA_4 and MeJA concentrations progressively decreased over time (Fig. 3c, d).

Comparative analysis shows that at all sampling stages, the concentrations of ABA, GA_3, GA_4, ZR, IPA, and DHZR were consistently higher in the HB cultivar than in the HL cultivar. Specifically, the ABA levels in HB were higher than in HL across all three stages, with concentrations in HB ranging between 150–200 ng/g FW, while those in HL remained between 100–150 ng/g FW. A notable exception was observed in November 2022, when the HL cultivar exhibited elevated levels of MeJA, BR, and IAA compared to the HB cultivar. Specifically, MeJA levels in HB showed an initial decrease followed by an increase as cold stress intensified, reaching approximately 36 ng/g FW by January, whereas in HL, they exhibited a declining trend. Both HB and HL showed an initial increase followed by a decrease in BR levels as cold stress progressed; the peak level in HB reached over 7 ng/g FW, while in HL it was only about 5 ng/g FW. However, the phytohormone concentrations in the other two stages were still higher in the HB cultivar (Fig. 3a–i).

Transcriptome sequencing overview

The length distributions of Unigene, CDS, and protein sequences collectively reflect key structural and functional features of the transcriptome. Most Unigenes are short, with the highest abundance in the 300–400 nt range, decreasing gradually as length increases, though a slight rebound occurs beyond 3,000 nt (Fig. 4a). Similarly, the CDS length distribution follows a declining trend as sequence length increases, with a steep drop in frequency observed among shorter sequences before leveling off into a slower descent. Toward the tail end, there is a slight uptick in CDS counts (Fig. 4b). Meanwhile, the protein sequence length distribution displays a distinct 'high left, low right' pattern, where short protein sequences vastly outnumber longer ones, and their frequency drops sharply as length increases (Fig. 4c).

Statistical analysis of Unigene annotation

COG organizes prokaryotic orthologs into 26 categories, while KOG performs a similar classification for eukaryotes (4,852 groups) (Table 3). The expanded eggNOG database integrates these frameworks with additional viral proteins. Pfam employs HMM modeling to characterize protein domains, and GO standardizes gene function classification through three ontologies (Molecular

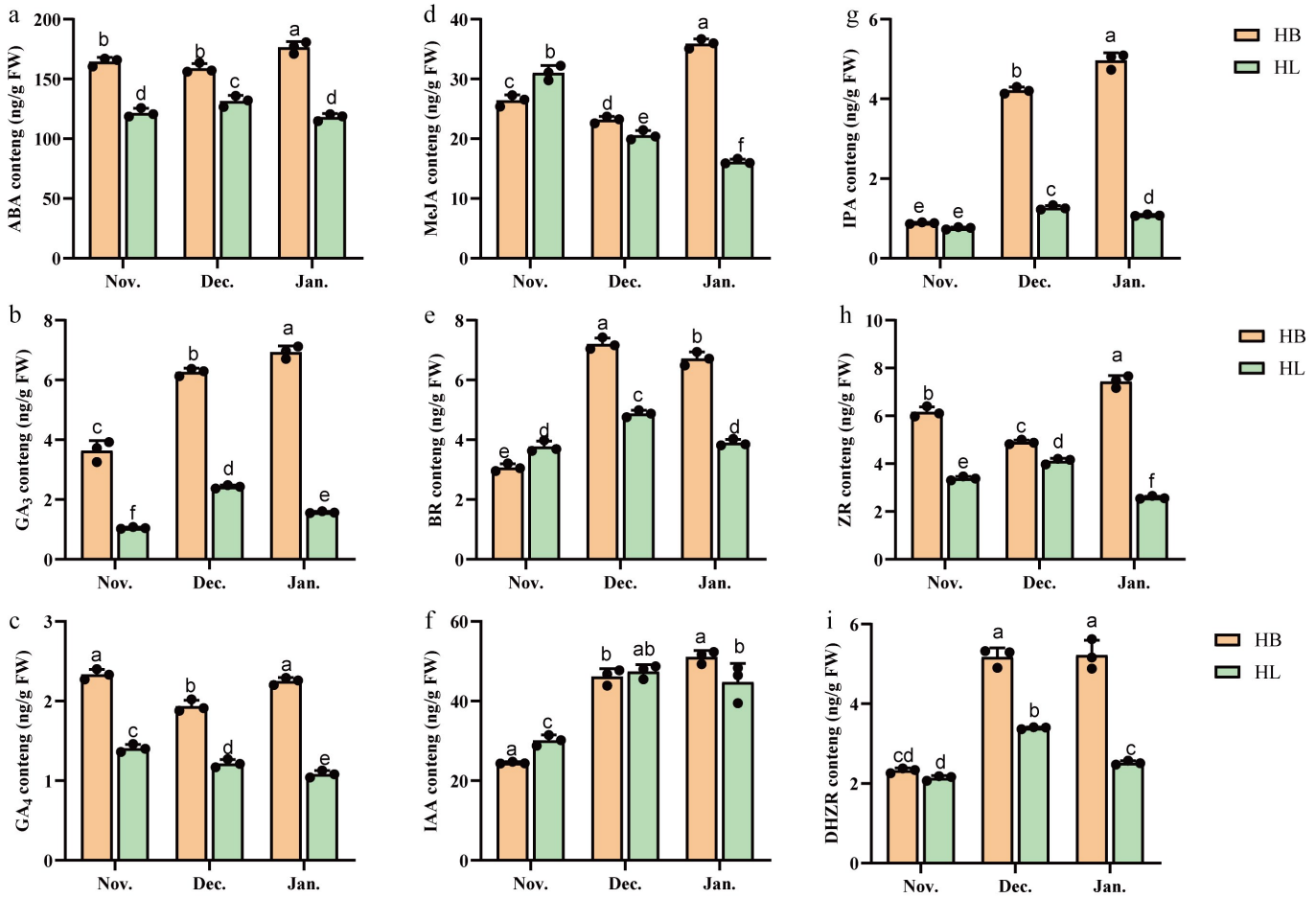

Fig. 3 Hormone content in three periods in 'Hang Baishao' (HB) and 'Hongling Chijin' (HL) under cold stress. (a) ABA content. (b) GA_3 content. (c) GA_4 content. (d) JA content. (e) BR content. (f) IAA content. (g) IPA content. (h) ZR content. (i) DHZR content. Different lowercase letters above the bars of Fig. 3a–i show significant differences at the 0.05 probability level; n = 3.

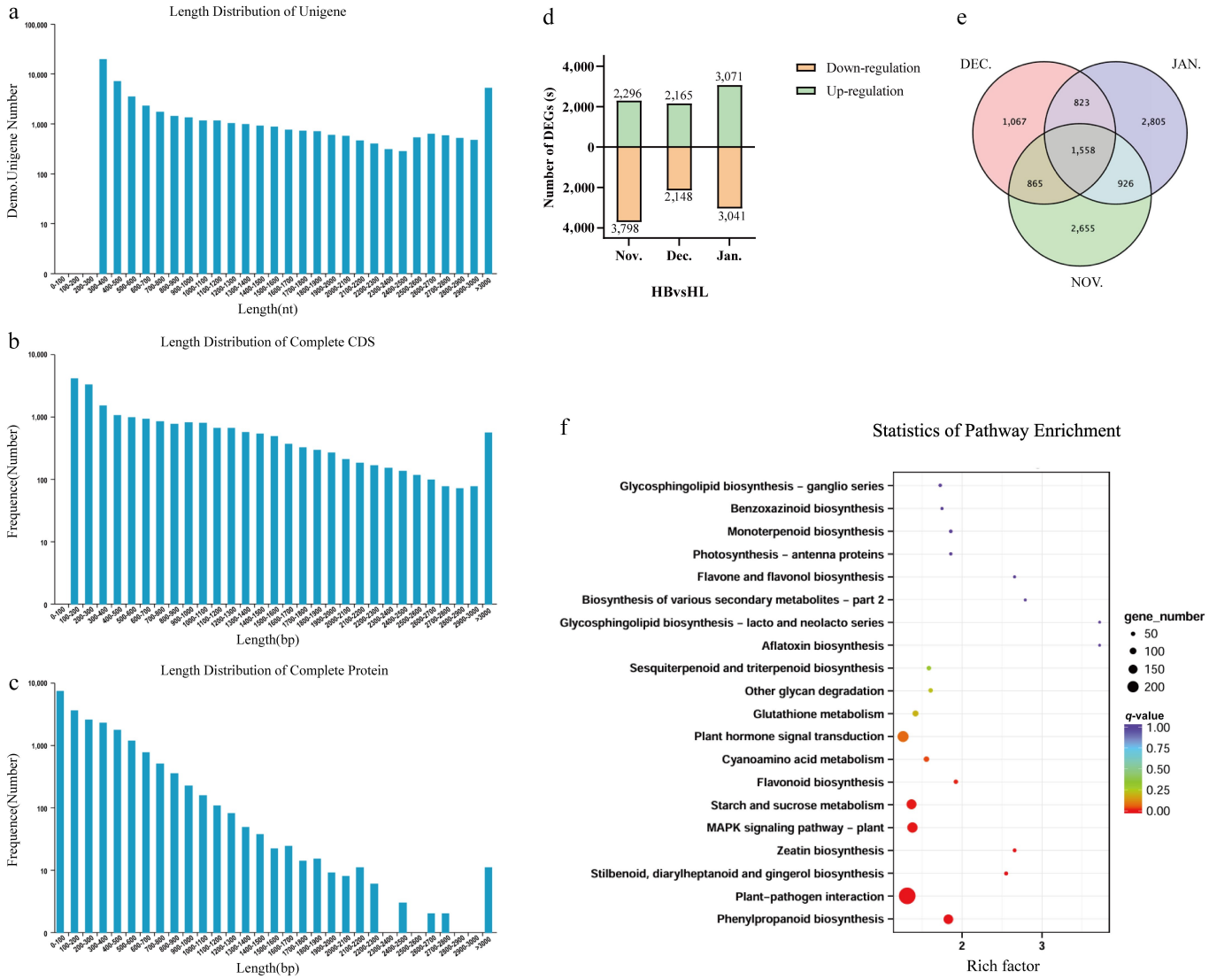

Fig. 4 Statistics and functional analysis of DEGs in HB and HL transcriptome during the winter of Harbin. (a) Length distribution of Unigene. (b) Length distribution of complete CDS. (c) Length distribution of complete protein. (d) Number of DEGs in three periods of HB and HL under cold stress. (e) Venn diagram of DEGs in three periods of HB and HL under cold stress. (f) KEGG enrichment of DEGs.

Function, Cellular Component, Biological Process). Finally, KEGG enables systems-level analysis by mapping gene products to biological pathways and networks (Table 3).

Identification and KEGG enrichment of DEGs

DEGs between two cultivars at various stages were screened from the transcriptome and subjected to the Venn analysis. The November sampling period showed the highest downregulation number among all stages, with 2,296 upregulated vs 3,798 downregulated genes identified from the total 6,094 DEGs detected between HB and HL cultivars. While in January, 6,112 DEGs were identified between HB and HL, including 3,071 upregulated and 3,041 downregulated genes, representing the highest upregulated number among all stages (Fig. 4d). Cross-comparison across three stages revealed 1,558 overlapping DEGs (Fig. 4e). A total of 10,700 DEGs (differentially expressed genes) were further analyzed, while stage-specific DEGs proved more numerous in January (2,805) and November (2,655), significantly exceeding December's count (1,067). KEGG enrichment analysis demonstrates significant enrichment in pathways including the starch and sucrose metabolism, Plant-pathogen interaction, Plant hormone signal transduction, MAPK signaling pathway-plant, and Zeatin biosynthesis (Fig. 4f). These findings would appear to suggest that herbaceous peony responds to cold stress through coordinated regulation of multiple biological processes and metabolic pathways.

Table 3. Statistics of Unigene annotation.

Anno_database	Annotated number	300 ≤ length	length ≥ 1,000
COG_Annotation	7,083	2,043	5,040
GO_Annotation	23,472	10,166	13,301
KEGG_Annotation	18,798	7,536	11,262
KOG_Annotation	15,395	6,023	9,372
Pfam_Annotation	18,418	5,915	12,503
Swissprot_Annotation	17,014	5,811	11,203
TrEMBL_Annotation	28,594	12,928	15,666
eggNOG_Annotation	23,573	9,933	13,640
nr_Annotation	29,753	14,007	15,746
All_Annotated	30,838	14,889	15,944

Validation of several key DEGs' expression

Based on the functional annotation, nine candidate genes associated with sugar metabolism (Fig. 5a–c), ROS regulation (Fig. 5d–f), and phytohormone signaling (Fig. 5g–i), were selected for the validation of expression by qRT-PCR. The concordance between qPCR-derived expression patterns and transcriptomic expression profiles (Fragments Per Kilobase of exon per Million mapped reads, FPKM) confirmed the reliability of sequencing results. These nine candidate genes are closely associated with some important physiological regulation under extremely cold stress, so they will be subjected to further in-depth analysis in subsequent discussions.

As cold stress intensified, the expression levels of *APL3*, *BMY3*, *GBSS1*, and *GRXS17* consistently increased in both HB and HL, with significantly higher expression observed in HL compared to HB, indicating their positive roles in responding to cold stress (Fig. 5a–c, e). In contrast, although *MSD1* expression rose with decreasing temperature, its levels were significantly higher in HB than in HL. While *IAA9* expression declined with temperature, it remained significantly higher in HL than in HB; meanwhile, the expression profiles of *GSH2*, *SPY*, and *ABF3* displayed irregular and non-directional shifts across temperature regimes, showing no clear correlation with stress intensity or cultivar-specific resilience (Fig. 5d, f–i). These divergent and often contradictory patterns suggest that the functional contributions of *MSD1*, *IAA9*, *GSH2*, *SPY*, and *ABF3* to cold stress adaptation are likely complex and context-dependent, warranting further mechanistic investigation (Table 4).

Clustering of DEGs and analysis of enriched KEGG pathways

To further explore the expression patterns of DEGs in HB and HL during the three periods, all DEGs were divided into four clusters, presenting four trends (Fig. 6): with the temperature drop, Cluster 1 was highly expressed in HB, where it increased, but showed no significant change in HL. Cluster 2 increased and was highly expressed in HL, but showed no significant change in HB. Cluster 3 decreased in both HB and HL, but was highly expressed in HB. Cluster 4 decreased in both HB and HL, but was highly expressed in HL.

The KEGG analysis of each cluster shows Cluster 1 is significantly enriched in plant-pathogen interaction, environmental adaptation, protein families: signaling and cellular processes; Cluster 2 is significantly enriched in the environmental information process pathway; Cluster 3 is significantly enriched in the carbohydrate metabolism, metabolism, and phenylpropanoid biosynthesis pathways; Cluster 4 is significantly enriched in the DNA replication proteins and biosynthesis of other secondary metabolism pathways (Fig. 6).

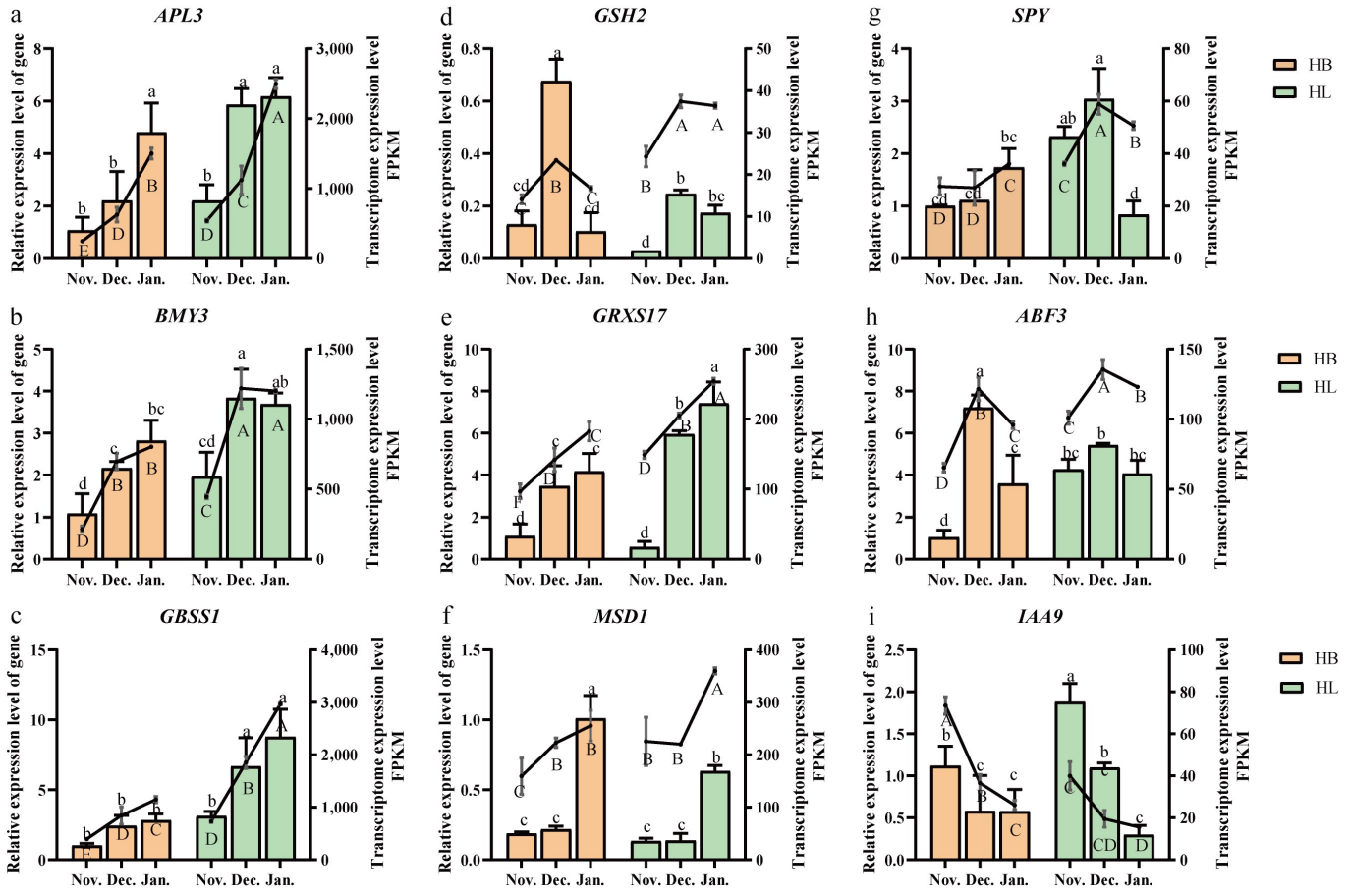

Fig. 5 The qRT-PCR analysis and transcriptomic expression of cold-tolerance related genes in 'Hang Baishao' (HB) and 'Hongling Chijin' (HL). (a) *APL3*. (b) *BMY3*. (c) *GBSS1*. (d) *GSH2*. (e) *GRXS17*. (f) *MSD1*. (g) *SPY*. (h) *ABF3*. (i) *IAA9*. The bar chart represents the gene relative expression level, and the line chart represents the transcriptome expression level. FPKM: Fragments per kilobase of exon model per million mapped reads. Different lowercase letters above the bars of Fig. 5a–i show significant differences at the 0.05 probability level; n = 3.

Table 4. qRT-PCR validation of candidate genes.

Gene name	Full name	HB vs HL	Nov. vs Dec. vs Jan.	Potential function
APL3		HL↑	Jan.↑	Positive
BMY3	*BETA-AMYLASE 3*	HL↑	Dec. or Jan.↑	Positive
GBSS1	*granule bound starch synthase 1*	HL↑	Jan.↑	Positive
GSH2	*GLUTATHIONE SYNTHETASE 2*	HB↑	Dec. ↑	Uncertain
GRXS17	*Arabidopsis thaliana monothiol glutaredoxin 17*	HL↑	Jan.↑	Positive
MSD1	*ARABIDOPSIS MANGANESE SUPEROXIDE DISMUTASE 1*	HB↑	Jan.↑	Uncertain
SPY	*SPINDLY*	HL↑	Dec. or Jan.↑	Uncertain
ABF3	*ABSCISIC ACID RESPONSIVE ELEMENTS-BINDING FACTOR 3*	HL↑	Dec. ↑	Uncertain
IAA9	*INDOLE-3-ACETIC ACID INDUCIBLE 9*	HL↑	Nov. ↑	Uncertain

'HL↑' means the gene expression level of 'Hongling Chijin' HL is higher than 'Hang Baishao' HB; 'HB↑' means the gene expression level of HB is higher than HL; 'Nov.↑' means the gene expression level in Nov. is higher than the other two months overall. 'Dec.↑' means the gene expression level in Dec. is higher than the other two months overall. 'Jan.↑' means the gene expression level in Jan. is higher than the other two months overall. 'Potential function' means the possible function of a gene in the regulation of cold stress of herbaceous peony.

Screening the key modules involved in herbaceous peony's response to cold stress based on the WGCNA

To further determine the specific modules and genes related to cold resistance-related traits between HB and HL, a WGCNA analysis was conducted. This analysis combined transcriptome sequencing data with 14 physiological indicators. These indicators, which included levels of soluble sugar, antioxidant enzyme activity, and phytohormone contents, were obtained from previous observations (Figs 2g–k, 3). Results show that 21 different modules were obtained. Analysis of the relationship between the module characteristic genes and physiological parameters related to cold resistance indicate that ME black is significantly positively correlated with POD, SOD, PRO, ABA, GA3, ZR, GA4, and IPA; while ME green-yellow is significantly negatively correlated with solution protein, POD, SOD, PRO, ABA, IAA, GA_3, BR, DHZR, and IPA (Fig. 7).

Expression of key genes in two modules and genes related to the aforementioned physiological and biochemical indicators

Figure 8 highlights some key candidate genes selected from two modules for further investigation. Ten genes with the highest average expression levels were selected from the Me black and Me green-yellow modules, respectively (Fig. 8). These genes were annotated as *XERO1*, *GSTU9*, *LEA14*, *NADP-ME4*, *TRA2*, etc., which may play key roles in regulating the cold resistance of herbaceous peony cultivars (Table 5).

Notably, highly expressed genes, including *XERO1* (a dehydrin gene), *MT3* (limiting oxidative damage), and *LTI65* (a low-temperature-responsive protein gene), are all functionally associated with plant stress responses, particularly cold acclimation, though exhibiting distinct expression dynamics. The sustained high expression of *XERO1* is consistent with a role in basal protection, likely contributing to cellular stability under cold stress. Whereas the induction of *LTI65* likely represents a targeted response to cold-induced dehydration. While the expression of *XERO1* and *LTI65* was elevated in HL compared to HB, implicating them as potential contributors to its strong cold tolerance, their expression patterns did not demonstrate a perfectly synchronized upward trend correlating with progressive decreases in temperature.

NADP-ME4 enhances the scavenging of active oxygen species by upregulating key antioxidant genes. In this study, *NADP-ME4* expression was consistently higher in HB than HL across all three sampling stages, suggesting that HB experienced greater oxidative stress under low temperatures, thereby triggering a stronger compensatory antioxidant response[32].

A similar expression pattern was observed for *MT3*, which was upregulated in both cultivars in response to increasingly low temperatures, with particularly high transcript levels observed in the buds of HB in January, indicating its close involvement in the peony's adaptation to cold stress. Contrary to expectations, however, its expression was significantly higher in the less cold-tolerant cultivar HB than in the more resilient HL. It may suggest its intense activation in the sensitive cultivar is a response to heightened oxidative damage. Given these intriguing expression profiles, further functional studies are warranted to elucidate the specific mechanisms underlying their roles in cold response.

Identifying crucial genes in the cold stress-related modules

To further investigate the cold tolerance-related genes within the two modules under both HB and HL conditions, a broadly targeted screening of the transcripts was performed. This screening focused on those associated with sugar and phytohormone signaling pathways to refine the analysis. These selected transcripts were then imported into Cytoscape to construct co-expression networks, where the degree value served as the primary metric for mapping interactions (Fig. 9). The top 15 genes by degree in each module were labeled to facilitate subsequent analysis and discussion (Table 6 and 7).

Notably, in the ME black module, *ANTHRANILATE SYNTHASE 2* (*ASA2*), a gene strongly associated with phytohormone signaling and involved in indole-3-acetic acid synthesis, stands out. Its central position suggests it may coordinate developmental adjustments under cold stress. Another significant gene in this module is *CHLOROPLAST-LOCALIZED SEC14-LIKE PROTEIN 1* (*CPSFL1*), which also shows strong connections to hormone signaling and functions as a negative regulator in the ABA signaling pathway, directly participating in hormonal response mechanisms. Two other genes with high degree values in this module were *AT5G55530* and *AT1G66860*, both of which lack annotation in The Arabidopsis Information Resource; however, their prominent network positions highlight them as promising candidates for future functional characterization. Additionally, DOF2.1, a DOF transcription factor containing a conserved zinc finger DNA-binding domain, was identified as another high-degree hub, suggesting its potential role as a key transcriptional regulator in the cold stress response.

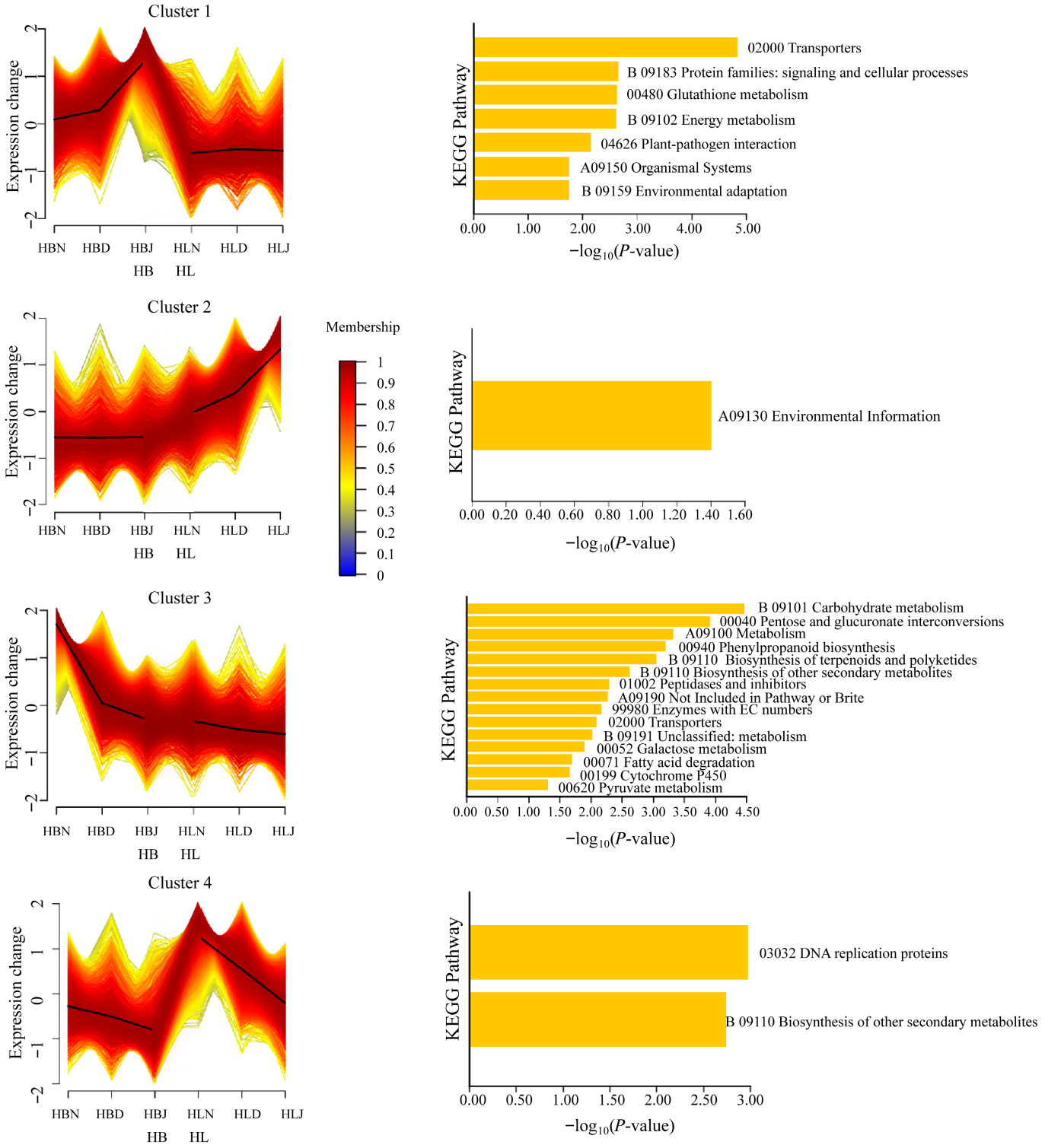

Fig. 6 Clustering and KEGG enrichment analysis of DEGs of HB and HL during the winter of Harbin; The x-axis labels represent cultivar names combined with sampling months, using the following nomenclature: HBN denotes the HB cultivar sampled in November (N), HBD indicates the HB cultivar in December (D), and HBJ corresponds to the HB cultivar in January (J). Similarly, HLN, HLD, and HLJ refer to the HL cultivar sampled in November, December, and January, respectively.

Within the ME yellowgreen module, the gene with the highest degree value is *WRKY DNA-BINDING PROTEIN 39* (*WRKY39*). This gene is a member of the WRKY transcription factor family and is a well-studied transcription factor gene known for its role in plant stress resistance. The *CHLOROPLAST GRPE 2* (*CGE2*) gene also ranked high in degree, suggesting its importance in chloroplast protein import and plastid-to-nucleus signaling during cold adaptation. The emergence of these highly connected hub genes suggests that cold tolerance in herbaceous peony may be coordinated through the integration of multiple synergistic mechanisms.

Discussion

Soluble sugar and protein probably increase the cold resistance of the herbaceous peony

The process of plant resistance to low-temperature stress is dually regulated by internal signals and external environmental changes. The generation and transmission of internal signals, as well as their regulation of cold resistance, are influenced by various elements such as sugars, proline, calcium ions, and protective proteins[6]. Soluble sugars are the primary substances for plant cold resistance. It functions to raise cellular osmotic potential and improve water retention, while also acting as a vital winter nutrient reserve that supports other physiological and biochemical processes essential for coping with low-temperature stress. The findings in iris (*Iris japonica*) demonstrate a dual role for sugar molecules as both signals and energy reserves in regulating growth transition through *IjFLCL1*-mediated pathways[33]. In addition, the content and conversion rate of starch during overwintering are closely associated with cold hardiness[34].

Meanwhile, cold treatment significantly increased soluble sugar content in both sugarcane (*Saccharum officinarum* L.) varieties (ROC22 and GT42), with GT42 showing greater accumulation and higher cold resistance than ROC22 at the bud stage[35]. Furthermore, salicylic acid treatment enhanced cold hardiness in *Magnolia wufengensis* by increasing soluble sugar accumulation, which improves freezing tolerance during natural cold acclimation[36]. In this study, HL demonstrated significantly superior morphological characteristics. These included longer bud length, greater plant height, larger crown width, increased stem number per plant, and higher flower count per individual. HL also has significantly higher soluble sugar content compared to HB, showing its stronger cold resistance, demonstrating the critical role of soluble sugars in mediating plant adaptive responses to cold stress (Fig. 2a–e, g). These results are consistent with previous studies conducted in sugarcane and *Magnolia wufengensis*[35,36]. The enriched starch and sucrose metabolism pathways likely facilitated increased soluble sugar levels through enhanced starch hydrolysis, thereby enhancing cold stress resistance in herbaceous peony.

Some studies suggest a positive correlation between increased protein content and plant cold resistance. A study demonstrated a positive correlation between increased soluble protein content and enhanced cold resistance in annual pitaya branches during 7 d cold stress[37]. Similarly, HB and HL exhibited an upward trend in soluble protein content under escalating cold stress, mirroring the response observed in annual pitaya shoots. However, this positive correlation does not hold consistently across all plant species and developmental stages. For example, the wheat of cold-sustainable genotypes maintained consistently high soluble protein levels both under optimal conditions and after cold exposure[38]. Also in this study, soluble protein content remained consistently high in both cultivars across stages, with HB slightly higher than HL (Fig. 2h). The results suggest that soluble proteins likely contributed to enhanced cold tolerance in both cultivars, but since no significant difference was observed between them, this parameter may not serve as a reliable indicator for evaluating and determining herbaceous peony cold resistance. The soluble protein content remained relatively stable in herbaceous peony, potentially due to increased synthesis of stress-resistant proteins and reduced production of other protein types through the MAPK signaling pathway.

Metabolism of antioxidant enzymes closely regulates the cold resistance of herbaceous peony

Plants accumulate excessive free radicals and ROS that damage membrane structures under various stresses[4]. SOD and POD are primary antioxidant enzymes, while PRO acts both as a ROS scavenger and an osmotic regulator to prevent cellular dehydration. In this study, both HB and HL showed increased SOD/POD activities and PRO content under cold stress. However, HB demonstrates significantly higher SOD/POD activities and greater PRO content than HL across all stages (Fig. 2i–k). Interestingly, studies on banana (*Musa* spp.) revealed that while PRO content increased in all cultivars during chilling, cold-tolerant banana varieties accumulated less PRO than cold-sensitive ones[39]. This observation shows a certain similarity with the findings of the present study. This similarity may suggest that HB, with lower cold tolerance compared to HL, experiences more pronounced oxidative damage.

Regulation of traditional phytohormones in cold tolerance of herbaceous peony

The five major traditional phytohormones, namely ABA, auxin, gibberellin, cytokinin, and ethylene, are critically involved in plant resistance to cold stress and other environmental challenges. ABA, a core phytohormone in cold stress, activates cold acclimation and enhances key stress-mitigating components, including proline, soluble proteins, and SOD activity[40,41]. Exogenous application of ABA has been shown to significantly enhance cold tolerance in cucumber (*Cucumis sativus* L.)[41]. Similarly, studies in Bermudagrass (*Cynodon dactylon* (L). Pers.) demonstrate that ABA treatment effectively strengthens cold stress tolerance, particularly in cold-resistant cultivars[42]. Moreover, ABA has been found to interact with other phytohormones, such as strigolactones and brassinosteroids, to positively regulate cold tolerance in tomato[43]. ABA content remained consistently high in both HB and HL cultivars, suggesting its critical role in the low-temperature stress response of herbaceous peony (Fig. 3a).

Auxins play a key role in cold stress responses. For example, overexpression of microRNA393 improved cold tolerance and tillering of switchgrass (*Panicum virgatum* L.) through regulation of auxin signaling transduction[44]. Building on prior evidence of auxin's role in cold adaptation, the analysis of HB and HL reveals that their hormonal dynamics also operate through auxin pathways. Specifically, this study revealed that IAA, IPA, and DHZR showed sustained increases in HB, but followed an initial rise, followed by a decline in HL, consistent with cold adaptation traits (Fig. 3f, g, i). This implies that both cultivars responded to cold stress through substantial increases in cytokinins and auxins, with HL exhibiting stronger cold resistance by ultimately reducing these phytohormones after initial elevation.

Meanwhile, in HL, GA_3 first increased then decreased, whereas in HB, GA_3 consistently rose and was significantly higher than in HL (Fig. 3b). This confirms that HL enhances cold resistance by suppressing GA signaling, representing a strategic balance between growth and stress adaptation.

Regulation of novel phytohormones in cold tolerance of herbaceous peony

In addition to the traditional five major classes of phytohormones, the scientific community has identified a variety of novel phytohormones over recent decades, such as JA, BR, salicylic acid, and

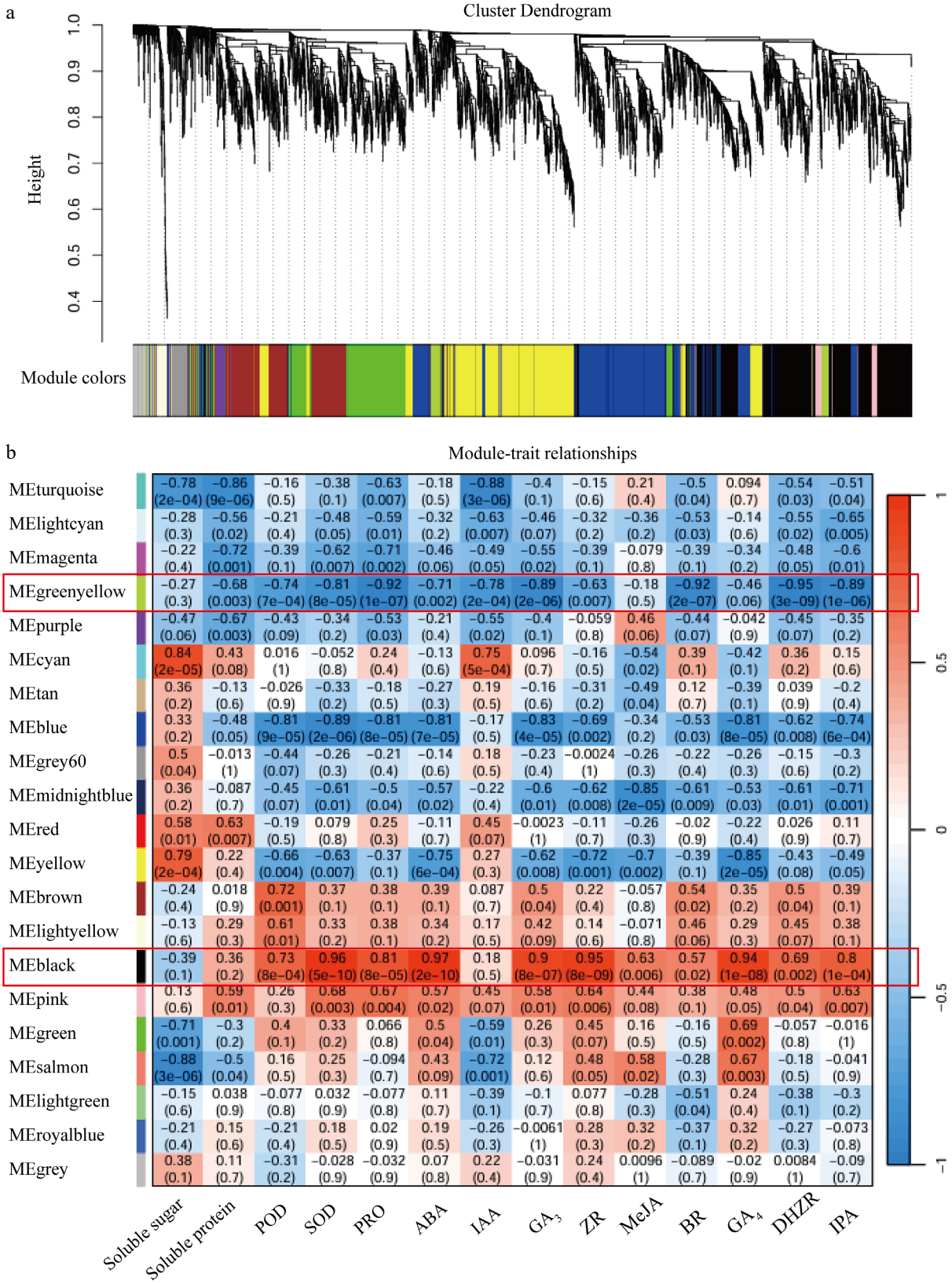

Fig. 7 WGCNA analysis. (a) Cluster dendrogram. (b) Module-trait relationships.

strigolactones, all of which have been demonstrated to play significant roles in enhancing plant resistance to cold and other environmental stresses. Furthermore, exogenous MeJA significantly promoted cold tolerance of tomato[45]. Experimental studies demonstrate that exogenous jasmonates (JAs) enhance cold tolerance in blood orange (*Citrus sinensis* L. Osbeck)[46]. This data showed JA content continuously decreased in HL but exhibited an initial decline followed by an increase in HB, suggesting JA plays a

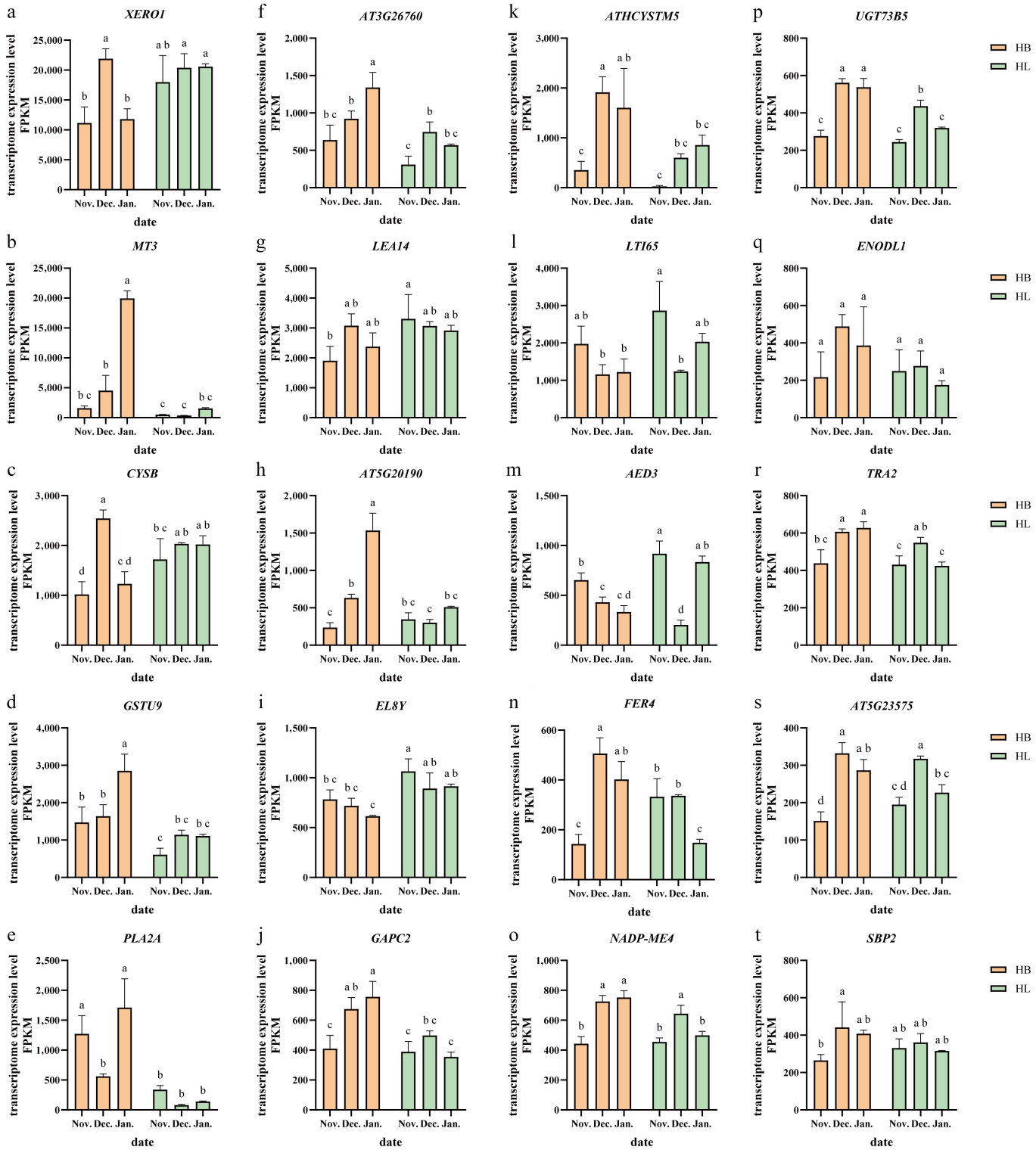

Fig. 8 Transcriptome expression levels of genes potentially involved in cold stress response are shown for 'Hang Baishao' (HB) and 'Hongling Chijin' (HL). (a)–(j) Genes from Me black modules, and (k)–(t) Me greenyellow modules are displayed in the left and right panels, respectively. Different lowercase letters above the bars of (a)–(t) show significant differences at the 0.05 probability level; $n = 3$.

prominent role in the early cold stress phase before diminishing over time in HL (Fig. 3d).

BR, a natural stress mitigator, exhibits dual functions in growth regulation and abiotic stress protection. For instance, BR activates the ascorbate-glutathione cycle through an ABA-independent regulatory system, scavenging excess ROS under cold stress in grapevine (*Vitis vinifera* L.), thereby enhancing their cold resistance[47]. Sodium nitrophenate plays a role in mediating the BR signal to regulate the cold tolerance of cucumber (*Cucumis sativus* L.)[48]. BR content in both HB and HL initially increased, then declined, peaking during early cold stress before decreasing temporally (Fig. 3e). This response pattern is not unique; under cold stress, BR levels in

Table 5. Summary of gene abbreviations, full names, and functions.

Abbreviations	Full name	Function
XERO1	*DEHYDRIN XERO 1*	Dehydrin
MT3	*METALLOTHIONEIN 3*	Limiting oxidative damage
CYSB	*ARABIDOPSIS THALIANA PHYTOCYSTATIN 6*	Encodes a protein with cysteine proteinase inhibitor activity
GSTU9	*glutathione S-transferase tau 9*	Encodes glutathione transferase belonging to the tau class of GSTs
PLA2A	*PHOSPHOLIPASE A 2A*	Contributes to resistance to virus
AT3G26760		NAD(P)-binding Rossmann-fold superfamily protein
LEA14	*LATE EMBRYOGENESIS ABUNDANT 14*	Encodes late-embryogenesis abundant protein
AT5G20190		Tetratricopeptide repeat (TPR)-like superfamily protein
EL8Y	*RIBOSOMAL PROTEIN EL8Y*	Ribosomal protein L7Ae/L30e/S12e/Gadd45 family protein
GAPC2	*GLYCERALDEHYDE-3-PHOSPHATE DEHYDROGENASE C2*	The expression level is upregulated in Arabidopsis seedlings exposed to cadmium
ATHCYSTM5	*CYSTEINE-RICH TRANSMEMBRANE MODULE 5*	Cysteine-rich/transmembrane domain A-like protein
LTI65	*LOW-TEMPERATURE-INDUCED 65*	Encodes a protein that is induced in expression in response to water deprivation such as cold
AED3	*APOPLASTIC EDS1-DEPENDENT 3*	Eukaryotic aspartyl protease family protein
FER4	*ferritin 4*	Encodes FERRITIN 4, AtFER4
NADP-ME4	*NADP-malic enzyme 4*	Localized to chloroplasts and expressed throughout the whole plant and during embryogenesis and germination, limiting oxidative damage
UGT73B5	*UDP-glucosyl transferase 73B5*	Involved in response to insect oral secretions
ENODL1	*early nodulin-like protein 1*	Early nodulin-like protein 1
TRA2	*TRANSALDOLASE 2*	Transaldolase which contributes to ROS homeostasis in response to Glc during early seedling growth
AT5G23575		Transmembrane CLPTM1 family protein
SBP2	*SELENIUM-BINDING PROTEIN 2*	Selenium-binding protein 2

The information presented in this table was obtained from the publicly available Arabidopsis Information Resource website at www.arabidopsis.org.

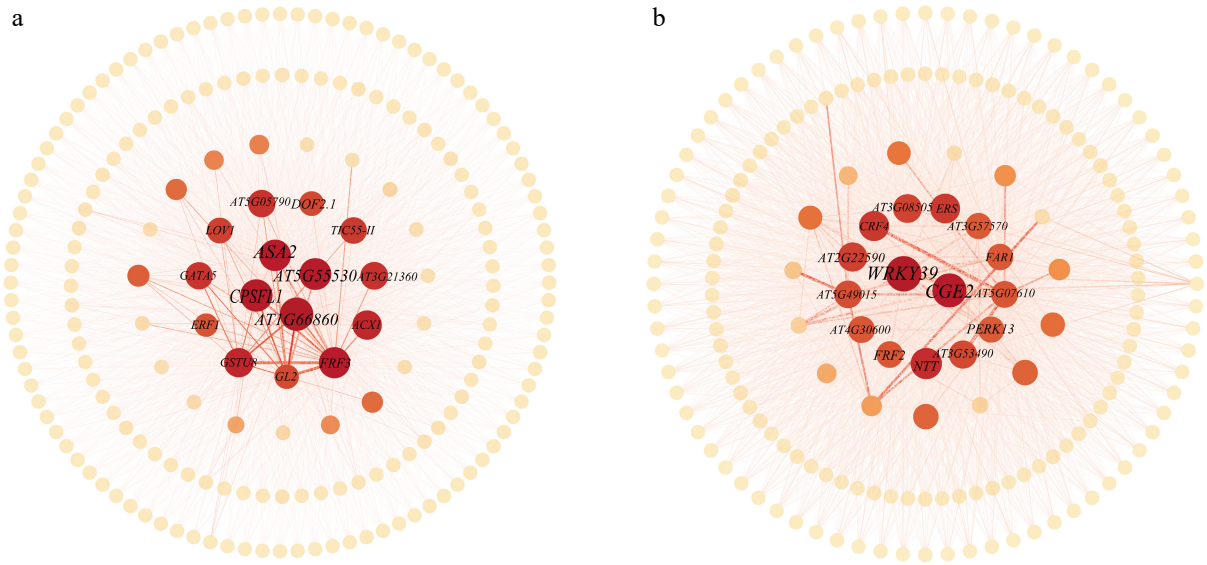

Fig. 9 Co-expression networks of important genes in the (a) ME black, and (b) ME yellowgreen modules. In the network visualization, both the size and color intensity of each gene node are determined by its degree value. Larger node sizes and darker colors represent higher degree values.

grapevine, HB, and HL all exhibited a similar trend: an initial increase to a peak, followed by a subsequent decline.

Regulation of cold adaptation by key genes involved in sugar metabolism, ROS regulation, and phytohormone signaling

Plants employ diverse molecular strategies to enhance cold tolerance, involving key genes that regulate sugar metabolism, redox homeostasis, and phytohormone signaling. Specifically, *APL3* in *Spirodela polyrhiza* promotes starch accumulation to support turion formation and energy storage[49]. While *BMY3* in rhubarb (*Rheum rhabarbarum* L. Polygonacea family) facilitates starch-to-sugar conversion to enable dormancy release and cold adaptation[50]. *GSH2* enhances chilling tolerance in species like tomato by synthesizing glutathione to mitigate oxidative stress, dependent on energy availability and regulatory cascades. Similarly, *GRXs* in tea plant (*Camellia sinensis* (L.) Kuntze) and banana (*Musa* acuminata) maintain redox balance under low-temperature stress, with members like *MaGRX17* specializing in antioxidative defense[51,52]. *APL3*, *BMY3*, and *GRXS17* all exhibited increased expression levels in both HL and HB under progressively severe cold stress, with even higher expression observed in the more cold-tolerant cultivar HL (Fig. 5a, b, e). This indicates their active roles in responding to cold stress, consistent with the functions of their orthologs in *Spirodela polyrhiza*, rhubarb, banana, tomato, rice, and tea plant[49–52].

In contrast, *MSD1* is down-regulated across *Arabidopsis* ecotypes under cold conditions, suggesting context-specific roles[53].

Table 6. Summary of gene abbreviations, full names, and functions in the ME black module.

Abbreviations	Full name	Function
ASA2	*ANTHRANILATE SYNTHASE 2*	Expression was not induced by wounding nor bacterial pathogen infiltration
CPSFL1	*CHLOROPLAST-LOCALIZED SEC14- LIKE PROTEIN*	Sec14p-like protein involved in chloroplast vesicle transport and required for photoauxotrophic growth
AT1G66860		Class I glutamine amidotransferase-like superfamily protein
AT5G55530		Calcium-dependent lipid-binding family protein
GSTU8	*glutathione S-transferase TAU 8*	Encodes glutathione transferase belonging to the tau class of GSTs
FRF3	*FAR1-RELATED SEQUENCES-RELATED FACTOR3*	Encodes one of four FRS factor-like genes in Arabidopsis
ACX1	*ACYL-COA OXIDASE 1*	Encodes a medium to long-chain acyl-CoA oxidase
GATA5	*GATA TRANSCRIPTION FACTOR 5*	Involved in regulating carbon and nitrogen metabolism
AT5G05790		Duplicated homeodomain-like superfamily protein
AT3G21360		2-oxoglutarate (2OG) and Fe(II)-dependent oxygenase superfamily protein
DOF2.1	*DOF PROTEIN 2.1*	DOF transcription factor with a conserved zinc finger (ZF) DNA-binding domain
TIC55-II	*TRANSLOCON AT THE INNER ENVELOPE MEMBRANE OF CHLOROPLASTS 55-II*	Translocon at the inner envelope membrane of chloroplasts 55-II
ERF1	*ETHYLENE RESPONSE FACTOR 1*	Involved in ethylene signaling cascade
GL2	*GLABRA2*	A homeodomain protein affects epidermal cell identity including trichomes, root hairs, and seed coat
LOV1	*LOCUS ORCHESTRATING VICTORIN EFFECTS1*	A disease susceptibility gene

The information presented in this table was obtained from the publicly available Arabidopsis Information Resource website at www.arabidopsis.org.

Table 7. Summary of gene abbreviations, full names, and functions in the ME yellowgreen module.

Abbreviations	Full name	Function
WRKY39	*WRKY DNA-BINDING PROTEIN 39*	Member of WRKY Transcription Factor; Group II-d
CGE2	*CHLOROPLAST GRPE 2*	Chloroplast GrpE protein
NTT	*NO TRANSMITTING TRACT*	Involved in transmitting tract development and pollen tube growth
CRF4	*CYTOKININ RESPONSE FACTOR 4*	Encodes a member of the ERF subfamily B-5 of ERF/AP2 transcription factor family
AT3G08505		Zinc finger family protein
ERS	*ETHYLENE RESPONSE SENSOR 1*	Ethylene receptor, subfamily 1 and has histidine kinase activity
AT2G22590		UDP-Glycosyltransferase superfamily protein
AT5G49015		Expressed protein
AT4G30600		Signal recognition particle receptor alpha subunit family protein
FRF2	*FAR1-RELATED SEQUENCES-RELATED FACTOR2*	Encodes one of four FRS factor-like genes in Arabidopsis
AT3G53490		Valine-tRNA ligase
PERK13	*Proline-rich extensin-like receptor kinase 13*	Modulates phosphate deficiency-induced root hair elongation
AT5G07610		F-box family protein
FAR1	*FATTY ACID REDUCTASE 1*	Are shown to generate the fatty alcohols found in root, seed coat, and wound-induced leaf tissue
AT3G57570		ARM repeat superfamily protein

The information presented in this table was obtained from the publicly available Arabidopsis Information Resource website at www.arabidopsis.org.

Meanwhile, *ABF3* in pear (*Pyrus pyrifolia* White Pear Group) integrates ABA and GA signaling to ensure winter survival and synchronized bud-break[54]. In Moso bamboo (*Phyllostachys edulis* [Carrière] J. Houz.), *IAA9* promotes stress adaptation via hypomethylation, which facilitates the integration of auxin signaling[55]. These mechanisms collectively underscore the complexity and species-specificity of plant cold adaptation; however, the coordinated regulatory functions of genes in response to cold stress require further elucidation.

Regulatory functions of key cold-responsive genes in herbaceous peony

The expression levels of *XERO1* and *LTI65* were higher in HL compared to HB, suggesting their potential functional importance in cold tolerance, though their precise mechanisms remain to be fully elucidated. Similarly, *MT3* enhances cold tolerance in banana (*Musa acuminata* Colla cv. Cavendish) through sustained antioxidant defense that mitigates oxidative damage under low temperature[56]. *NADP-ME4* enhances the expression of genes encoding superoxide dismutase, peroxidase, and pyrroline-5-carboxylate synthase, thereby boosting the plant's ability to scavenge ROS. This activity reduces the damage caused by cold stress[32]. The expression patterns of genes such as *XERO1*, *LTI65*, and *MT3* in HL and HB did not fully align with initial expectations, suggesting that their roles in responding to cold stress require further investigation (Fig. 8a, b, i).

By regulating the expression of target genes, WRKY transcription factors are increasingly recognized by emerging research as critical players in multiple facets of plant biology, from growth and development to adaptation to environmental stresses[57]. For example, a comparative genomic analysis of three *Pterocarya* species (specifically between *P. stenoptera* and *P. macroptera*), *WRKY39* was identified as a key cold-tolerance gene under environmental selection during the speciation of Pterocarya trees[58]. The specific functions of WRKY transcription factors in cold tolerance of herbaceous peony remain unclear; however, given the likely conservation of their regulatory pathways, a key objective is to identify how peony WRKYs integrate upstream cold-stress and hormone signaling to enhance cold tolerance. PCA and network analyses demonstrated *ASA2*'s effectiveness in enhancing cold tolerance by strengthening photosynthesis-antioxidant coordination. This treatment upregulated key genes, reducing oxidative damage and preserving chloroplast function in common bean (*Phaseolus vulgaris* L.)[59]. The function of these

genes in the cold stress response of herbaceous plants is yet to be explored, although their roles in cold tolerance have been preliminarily established in other species. In *Arabidopsis thaliana*, *CPSFL1* potentially facilitates vesicle formation by transferring lipids such as PIP and PtdOH, which are critical for thylakoid biogenesis and carotenoid transport. It is hypothesized that by maintaining the integrity of these photosynthetic components, *CPSFL1* may indirectly contribute to the plant's cold tolerance[60]. Future investigations could therefore focus on the synergistic relationships among these transcription factors and key genes to identify critical regulatory nodes within the cold tolerance network of herbaceous peony.

Conclusions

Physiological differences are consistent with HL's superior overwintering phenotypes compared to HB. Transcriptomic analysis revealed that differential gene expression in starch and sucrose metabolism, plant-pathogen interactions, and plant hormone signal transduction pathways in cold adaptation. Notably, genes such as *XERO1* (a dehydrin gene), *LTI65* (a low-temperature-responsive protein gene), *NADP-ME4* (involved in energy metabolism), *PLA2A* (*a lipid acyl hydrolase*), *WRKY39* (a member of the *WRKY* transcription factor), and *ASA2* (involved in plant hormone biosynthesis) were identified as potential key regulators for further functional investigation. The innovation lies in evaluating herbaceous peonies in the extreme cold of a major metropolitan area. Unlike controlled laboratory settings, this approach provides a more authentic assessment of frost damage. It also screened southern against local cultivars to identify cold-resilient varieties. This study establishes a foundation for elucidating the physiological mechanisms of cold stress adaptation in herbaceous peony and provides essential groundwork for future functional validation and interaction studies of cold tolerance-related genes.

Author contributions

The authors confirm contribution to the paper as follows: study conception and design, experimental planning: Zhang J, Liu Z, Xia Y; experimental guidance: Li D; experimental procedures: Shen Y, Wang Q, Shi X, Guo J, Chen X; data collection and analysis: Shen Y, Wang Q, Shi X, Li D; draft manuscript preparation: Shen Y, Wang Q; manuscript review: Zhang J, Li D; funding acquisition: Zhang J, Liu Z, Xia Y. All authors reviewed the results and approved the final version of the manuscript.

Data availability

All data generated or analyzed during this study are included in this published article.

Acknowledgments

This research was funded by the Science and Technology Research Project of Harbin (Grant No. 2021ZSZZNS05), the National Natural Science Foundation of China (NSFC, Grant No. 32371933), Zhejiang Provincial Natural Science Foundation of China (Grant No. LY23C160004), and the Zhejiang Province 'Three Rural Nine Parties' Science and Technology Cooperation Plan Project (Grant No. 2025SNJF039).

Conflict of interest

The authors declare that they have no conflict of interest.

Dates

Received 2 September 2025; Revised 1 December 2025; Accepted 16 December 2025; Published online 4 March 2026

References

[1] Tiwari M, Kumar R, Subramanian S, Doherty CJ, Krishna Jagadish SV. 2023. Auxin – cytokinin interplay shapes root functionality under low-temperature stress. *Trends in Plant Science* 28(4):447–459

[2] Mao Y, Ji X, Meng Q, Xu Z, Yuan Y, et al. 2022. Contribution of anthocyanin and polyunsaturated fatty acid biosynthesis to cold tolerance during bud sprouting in tree peony. *Industrial Crops and Products* 188:115563

[3] Wang X, Ding Y, Li Z, Shi Y, Wang J, et al. 2019. PUB25 and PUB26 promote plant freezing tolerance by degrading the cold signaling negative regulator MYB15. *Developmental Cell* 51:222–235

[4] Ding Y, Shi Y, Yang S. 2019. Advances and challenges in uncovering cold tolerance regulatory mechanisms in plants. *New Phytologist* 222(4):1690–1704

[5] Zhou X, Muhammad I, Lan H, Xia C. 2022. Recent advances in the analysis of cold tolerance in maize. *Frontiers in Plant Science* 13:866034

[6] Wang L, Guo Y, Yang S. 2021. Designed breeding for adaptation of crops to environmental abiotic stresses. *SCIENTIA SINICA Vitae* 51:1424–1434

[7] Ding Y, Shi Y, Yang S. 2024. Regulatory networks underlying plant responses and adaptation to cold stress. *Annual Review of Genetics* 58:43–65

[8] Qian ZZ, Zhuang SY, Li Q, Gui RY. 2019. Soil silicon amendment increases *Phyllostachys praecox* cold tolerance in a pot experiment. *Forests* 10(5):405

[9] Azarfam SP, Nadian H, Moezzi A, Gholami A. 2020. Effect of silicon on phytochemical and medicinal properties of *Aloe vera* under cold stress. *Applied Ecology and Environmental Research* 18:561–575

[10] Wang R, Yu M, Xia J, Ren Z, Xing J, et al. 2023. Cold stress triggers freezing tolerance in wheat (*Triticum aestivum* L.) via hormone regulation and transcription of related genes. *Plant Biology* 25(2):308–321

[11] Zhao Y, Zhou M, Xu K, Li J, Li S, et al. 2019. Integrated transcriptomics and metabolomics analyses provide insights into cold stress response in wheat. *The Crop Journal* 7:857–866

[12] Xu G, Li L, Zhou J, He M, Lyu D, et al. 2023. Integrated transcriptomics and metabolomics analyses reveal key genes and essential metabolic pathways for the acquisition of cold tolerance during dormancy in apple. *Environmental and Experimental Botany* 213:105413

[13] Xie X, Yang S, Zhao X, Shang T, Han X. 2025. Mechanisms of silicon-mediated amelioration for *Camellia sinensis* using physiology, transcriptomics, and metabolomics under cold stress. *Beverage Plant Research* 5:e003

[14] Shen C, Li D, He R, Fang Z, Xia Y, et al. 2014. Comparative transcriptome analysis of RNA-seq data for cold-tolerant and cold-sensitive rice genotypes under cold stress. *Journal of Plant Biology* 57(6):337–348

[15] Liao W, Xiao L, Hao X, Shan C, Zhou Z, et al. 2025. Physiological and transcriptomic analysis of two types of Hami melons in low-temperature storage. *Plants* 14(8):1153

[16] Guo X, Wei F, Jian H, Lian B, Dang X, et al. 2023. Systematic analysis of the NDR1/HIN1-like (NHL) family in *Gossypium hirsutum* reveals a role of *GhNHL69* in responding to cold stress. *Industrial Crops and Products* 206:117659

[17] Gan P, Luo X, Wei H, Hu Y, Li R, et al. 2024. Identification of hub genes that variate the *qCSS12*-mediated cold tolerance between *indica* and *japonica* rice using WGCNA. *Plant Cell Reports* 43(1):24

[18] Zhao D, Wei M, Shi M, Hao Z, Tao J. 2017. Identification and comparative profiling of miRNAs in herbaceous peony (*Paeonia lactiflora* pall.) with red/yellow bicoloured flowers. *Scientific Reports* 7:44926

[19] Sun J, Chen T, Wu Y, Tao J. 2021. Identification and functional verification of *PlFT* gene associated with flowering in herbaceous peony based on transcriptome analysis. *Ornamental Plant Research* 1:7

[20] Hao Z, Wei M, Gong S, Zhao D, Tao J. 2016. Transcriptome and digital gene expression analysis of herbaceous peony (*Paeonia lactiflora* Pall.) to screen thermo-tolerant related differently expressed genes. *Genes & Genomics* 38(12):1201−1215

[21] Tang Y, Xu H, Yu R, Lu L, Zhao D, et al. 2024. The SBP-box transcription factor PlSPL2 negatively regulates stem development in herbaceous peony. *Plant Cell Reports,* 43(12):275

[22] Wang Q, Li D, Guo J, Chen X, Cheng Y, et al. 2025. Physiological measurement and screening of key genes of the rhizome cold tolerance in the herbaceous peony cultivated over winter in Harbin. *Journal of Zhejiang University* 51(1):148−163. (in Chinese)

[23] Rhie YH, Jung HH, Kim KS. 2012. Chilling requirement for breaking dormancy and flowering in *Paeonia lactiflora* 'Taebaek', and 'Mulsurae'. *Horticulture, environment, and biotechnology* 53(4):277−282

[24] Wang X, Chen X, Zhang K, Li D, Shao L, et al. 2026. PlOBP1/PlDAM - *PlSOC1* module regulates bud dormancy transition in response to low temperature. *Plant, Cell & Environment* 49(1):334−351

[25] Walton EF, Mclaren GF, Boldingh HL. 2007. Seasonal patterns of starch and sugar accumulation in herbaceous peony (*Paeonia lactiflora* Pall.). *The Journal of Horticultural Science & Biotechnology* 82(3):365−370

[26] Zhao D, Luan Y, Xia X, Shi W, Tang Y, et al. 2020. Lignin provides mechanical support to herbaceous peony (*Paeonia lactiflora* pall.) stems. *Horticulture Research* 7:213

[27] Hussain S, Liu G, Liu D, Ahmed M, Hussain N, et al. 2015. Study on the expression of dehydrin genes and activities of antioxidative enzymes in floral buds of two sand pear (*Pyrus pyrifolia* Nakai) cultivars requiring different chilling hours for bud break. *Turkish Journal of Agriculture and Forestry* 39(6):930−939

[28] Li ZB, Zeng XY, Xu JW, Zhao RH, Wei YN. 2019. Transcriptomic profiling of cotton *Gossypium hirsutum* challenged with low-temperature gradients stress. *Scientific Data* 6:197

[29] Livak KJ, Schmittgen TD. 2001. Analysis of relative gene expression data using real-time quantitative PCR and the $2^{-\Delta\Delta CT}$ method. *Methods* 25(4):402−408

[30] Chen C, Chen H, Zhang Y, Thomas HR, Frank MH, et al. 2020. TBtools: an integrative toolkit developed for interactive analyses of big biological data. *Molecular Plant* 13(8):1194−1202

[31] Shannon P, Markiel A, Ozier O, Baliga NS, Wang JT, et al. 2003. Cytoscape: a software environment for integrated models of biomolecular interaction networks. *Genome Research* 13(11): 2498−2504

[32] Wen Z, Wang Y, Xia C, Zhang Y, Zhang H. 2021. Chloroplastic *SaNADP-ME4* of C_3–C_4 woody desert species *Salsola laricifolia* confers drought and salt stress resistance to *Arabidopsis*. *Plant* 10:1827

[33] Shao L, Xu T, Wang X, Chen X, Zhang R, et al. 2025. Sucrose-induced transcription factor IjSUSIBA2 fine-tunes growth transition through the *IjSVL2-IjFLCL1* module in evergreen Irises. *Plant, Cell & Environment* 48(12):8928−8946

[34] Liang G, Li Y, Wang P, Jiao S, Wang H, et al. 2022. *VaAPL1* promotes starch synthesis to constantly contribute to soluble sugar accumulation, improving low temperature tolerance in *Arabidopsis* and tomato. *Frontiers in Plant Science* 13:920424

[35] Huang X, Liang Y, Zhang B, Song X, Li Y, et al. 2022. Comparative transcriptome analysis reveals potential gene modules associated with cold tolerance in sugarcane (*Saccharum officinarum* L.). *Journal of Plant Growth Regulation* 41(7):2614−2628

[36] Duan X, Zhu Z, Yang Y, Duan J, Jia Z, et al. 2022. Salicylic acid regulates sugar metabolism that confers freezing tolerance in *Magnolia wufengensis* during natural cold acclimation. *Journal of Plant Growth Regulation* 41(1):227−235

[37] Zhou J, Wang L, Xiao T, Wang Z, Mao Y, et al. 2021. Physiological responses and proteomic analysis on the cold stress responses of annual pitaya (*Hylocereus* spp.) branches. *Journal of Chemistry* 2021:1416925

[38] Deryabin A, Zhukova K, Naraikina N, Venzhik Y. 2024. Effect of low temperature on content of primary metabolites in two wheat genotypes differing in cold tolerance. *Metabolites* 14(4):199

[39] Kosová K, Prášil IT, Vítámvás P, Dobrev P, Motyka V, et al. 2012. Complex phytohormone responses during the cold acclimation of two wheat cultivars differing in cold tolerance, winter Samanta and spring Sandra. *Journal of Plant Physiology* 169(6):567−576

[40] Li C, Pan Y, Cui J, Lu X, Yu W. 2025. Mechanism of ABA in plants exposed to cold stress. *Agronomy* 15(2):403

[41] Feng Q, Yang S, Wang Y, Lu L, Sun M, et al. 2021. Physiological and molecular mechanisms of ABA and $CaCl_2$ regulating chilling tolerance of cucumber seedlings. *Plants* 10(12):2746

[42] Huang X, Shi H, Hu Z, Liu A, Amombo E, et al. 2017. ABA is involved in regulation of cold stress response in bermudagrass. *Frontiers in Plant Science* 8:1613

[43] An S, Liu Y, Sang K, Wang T, Yu J, et al. 2023. Brassinosteroid signaling positively regulates abscisic acid biosynthesis in response to chilling stress in tomato. *Journal of Integrative Plant Biology* 65(1):10−24

[44] Liu Y, Wang K, Li D, Yan J, Zhang W. 2017. Enhanced cold tolerance and tillering in switchgrass (*Panicum virgatum* L.) by heterologous expression of *Osa-miR393a*. *Plant and Cell Physiology* 58(12):2226−2240

[45] Ding F, Wang X, Li Z, Wang M. 2023. Jasmonate positively regulates cold tolerance by promoting ABA biosynthesis in tomato. *Plants* 12(1):60

[46] Habibi F, Ramezanian A, Rahemi M, Eshghi S, Guillén F, et al. 2019. Postharvest treatments with γ -aminobutyric acid, methyl jasmonate, or methyl salicylate enhance chilling tolerance of blood orange fruit at prolonged cold storage. *Journal of The Science of Food and Agriculture* 99(14):6408−6417

[47] Wang Y, Ding S, Chen Z, Wang X, Jiang Q, et al. 2023. Transcriptomic analysis provides insights into the abscisic acid mediates brassinosteroid-induced cold resistance of grapevine (*Vitis vinifera* L.). *Plant Growth Regulation* 101(3):845−860

[48] Zhou M, Di Q, Yan Y, He C, Wang J, et al. 2025. Multi-omics reveal the molecular mechanisms of sodium nitrophenolate in enhancing cold tolerance through hormonal and antioxidant pathways in cucumber. *Plant Physiology and Biochemistry* 223:109836

[49] Wang W, Wu Y, Messing J. 2014. RNA-seq transcriptome analysis of spirodela dormancy without reproduction. *BMC Genomics* 15:60

[50] Wojtania A, Markiewicz M, Waligórski P. 2022. Regulation of the bud dormancy development and release in micropropagated rhubarb 'Malinowy'. *International Journal of Molecular Sciences* 23(3):1480

[51] Wang M, Ding F and Zhang S. 2020. Mutation of *SlSBPASE* aggravates chilling-induced oxidative stress by impairing glutathione biosynthesis and suppressing ascorbate-glutathione recycling in tomato plants. *Frontiers in Plant Science* 11:565701

[52] Li T, Li M, Jiang Y, Duan X. 2021. Genome-wide identification, characterization and expression profile of *glutaredoxin* gene family in relation to fruit ripening and response to abiotic and biotic stresses in banana (*Musa acuminata*). *International Journal of Biological Macromolecules* 170:636−651

[53] Jiang D, Yang W, Pi J, Yang G, Luo Y, et al. 2023. Genome-wide identification, characterization, and expression profiling of the *glutaredoxin* gene family in tea plant (*Camellia sinensis*). *Forests* 14(8):1647

[54] Yang Q, Wu X, Gao Y, Ni J, Li J, et al. 2023. PpyABF3 recruits the COMPASS-like complex to regulate bud dormancy maintenance via integrating ABA signaling and GA catabolism. *New Phytologist* 237:192−203

[55] Ding Y, Zou LH, Wu J, Ramakrishnan M, Gao Y, et al. 2022. The pattern of DNA methylation alteration, and its association with the expression changes of non-coding RNAs and mRNAs in Moso bamboo under abiotic stress. *Plant Science* 325:111451

[56] Liu J, Li F, Liang L, Jiang Y, Chen J. 2019. Fibroin delays chilling injury of postharvest banana fruit via enhanced antioxidant capability during cold storage. *Metabolites* 9(7):152

[57] Cheng Z, Luan Y, Meng J, Sun J, Tao J, et al. 2021. WRKY transcription factor response to high-temperature stress. *Plants* 10(10):2211

[58] Geng D, Liu M, Wang L, Zhang X, Ma J, et al. 2025. Genomic introgression underlies environmental adaptation in three species of Chinese wingnuts, *Pterocarya*. *Plant Diversity* 47(3):365–381

[59] Ali B, Kumar S, Sui X, Niu J, Yang J, et al. 2025. Exogenous acetylsalicylic acid mitigates cold stress in common bean seedlings by enhancing antioxidant defense and photosynthetic efficiency. *Frontiers in Plant Science* 16:1589706

[60] Hertle AP, García-Cerdán JG, Armbruster U, Shih R, Lee JJ, et al. 2020. A Sec14 domain protein is required for photoautotrophic growth and chloroplast vesicle formation in *Arabidopsis thaliana*. *Proceedings of the national academy of sciences of the united states of America* 117(16):9101–9111